Supplemental Information

- **Supplemental Figure 1. Validation of *Tbc1d8b*$^{\Delta 1}$.**
- **Supplemental Figure 2: Loss of *Tbc1d8b* affects nephrin localization and barrier permeability.**
- **Supplemental Figure 3: Microhomology-mediated end joining and localization of Tbc1d8b.**
- **Supplemental Figure 4: Effects of Rab5-RNAi for sequential tracer uptake.**
- **Supplemental Figure 5: Rab5- and Rab7-staining in Tbc1d8b-LOF and validation of Hrs knockdown and antibody..**
- **Supplemental Figure 6: Alignment of human, murine and *Drosophila Tbc1d8b* and coexpression with human *Rab11*.**
- **Supplemental Figure 7: Overexpression studies of murine Tbc1d8b.**
- **Supplemental Figure 8: Patient-derived mutations in *TBC1D8B*.**
- **Supplemental Table 1: Primer sequences.**

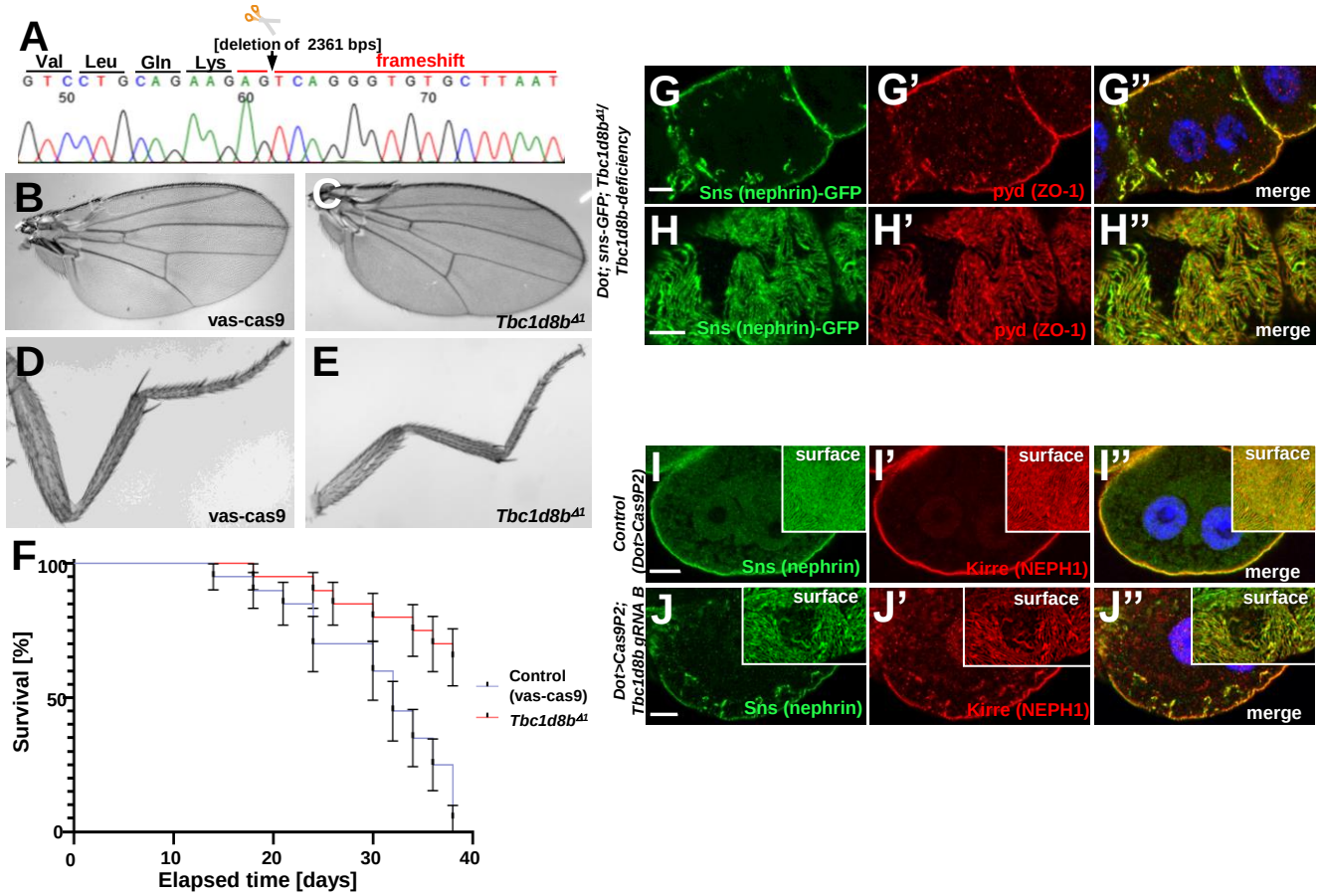

Supplemental Figure 1: Validation of *Tbc1d8b$^{\Delta 1}$*.

(A) Shown is a Sanger chromatograms of the region of *Tbc1d8b* that is deleted in *Tbc1d8b$^{\Delta 1}$*. The sequence following the indicated cutting site of the respective gRNA aligns 2,361 bp downstream beyond the cutting site of the second gRNA indicating the interjacent sequence was removed.

(B-C) Shown are *Drosophila* wings from control (vas-cas9) (B) vs. homozygous *Tbc1d8b$^{\Delta 1}$* flies (C). Wings are formed without overt phenotype in the mutant animals.

(D-E) Mounted legs from *Drosophila* are shown. Legs from homozygous *Tbc1d8b$^{\Delta 1}$* flies (E) show no structural anomaly compared to vas-Cas9 control (D).

(F) Survival of *Tbc1d8b$^{\Delta 1}$* animals is shown in comparison to vas-Cas9 as control.

(G-H'') Shown are cross sections (G-G'') and a tangential sections (H-H'') of nephrocytes that carry the *Tbc1d8b$^{\Delta 1}$* allele heterozygously over an independent deletion spanning several genes. The phenotype is comparable to the phenotype carrying *Tbc1d8b$^{\Delta 1}$* homozygously. This confirms that no second site mutation but the deletion of the *Tbc1d8b* locus is cause of the phenotype. Nephrin is visualized by knock-in of GFP into its genomic locus. Nuclei are marked by Hoechst 33342.

(I-J'') Nephrocytes after a conditional CRISPR/Cas9-mediated loss of Tbc1d8b using the same gRNAs employed to generate the stable deletion reveal a similar but more pronounced phenotype (J-J'') compared to control cells (Cas9 without gRNA, I-I'').

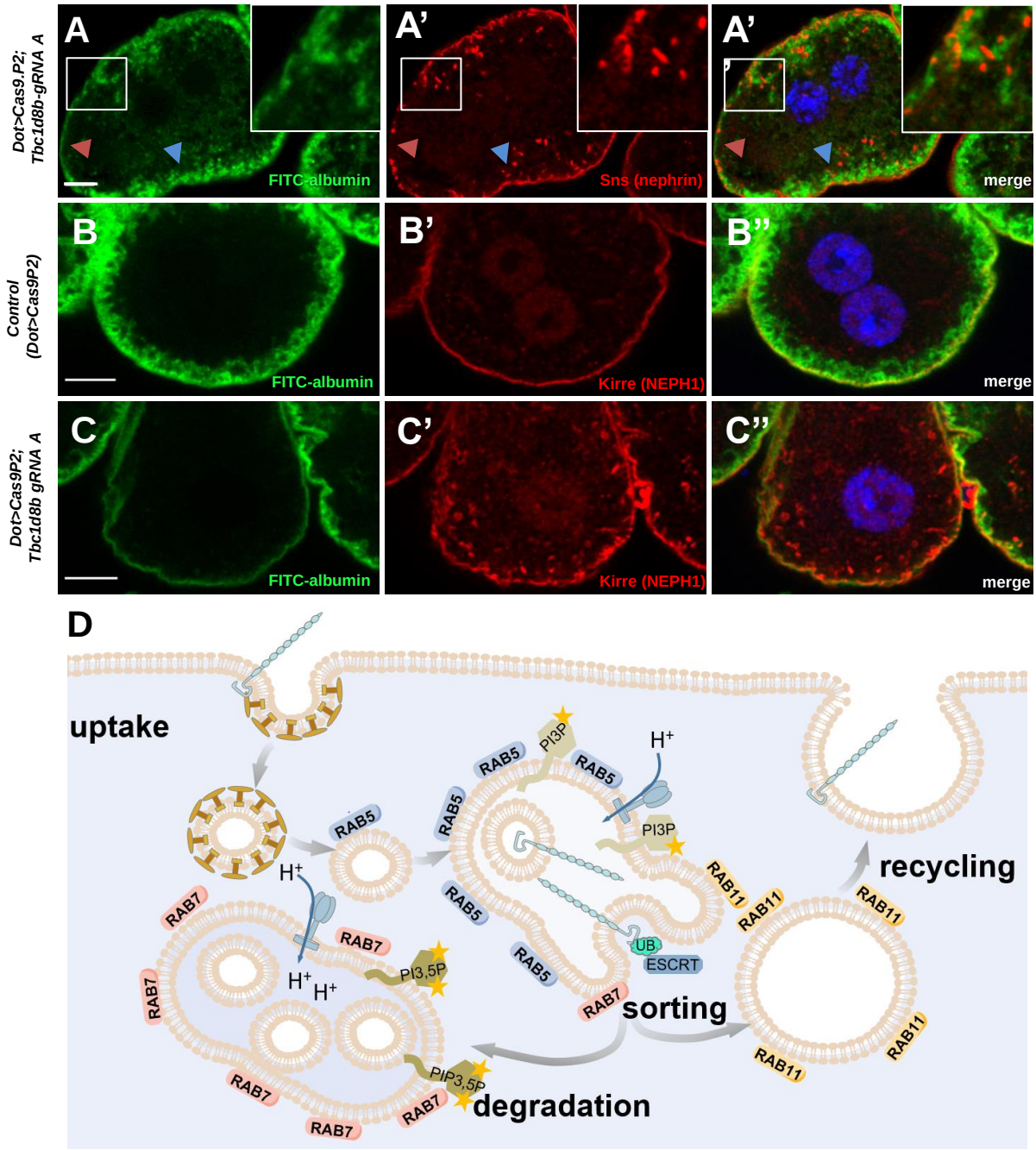

Supplemental Figure 2: Loss of *Tbc1d8b* affects nephrin localization and barrier permeability.
(A-A'') Nephrocytes with CRISPR/Cas9-mediated loss of Tbc1d8b were exposed extendedly to endocytic tracer FITC-albumin for 15 min ex vivo before fixation and nephrin (Sns) staining. The ectopic nephrin below the cell surface does not colocalize with the endocytic tracer (inset) and tracer endocytosis is diminished in surface sections lacking the slit diaphragm protein (red arrow head) compared to more intact sections (blue arrow head). Nuclei are marked by Hoechst 33342 in blue throughout the figure.
(B-C'') Confocal microscopy images of nephrocytes stained for Neph1 (green) together with labeling of the channels by FITC-albumin *via* passive diffusion after brief fixation. Channels extend below the surface, but are not filled upon loss of *Tbc1d8b*.
(D) Schematic illustrates endocytosis with the major Rab proteins. Rab5 promotes uptake and fusion of vesicles to form early endosomes as sorting stations. Early endosomes mature forming intraluminal vesicles and acidify. The ESCRT complex promotes formation of intraluminal vesicles. Rab11, also present in subdomains of early endosomes, promotes recycling back to the plasma membrane. Mature early endosomes increasingly form PI3P on their surface. The cascade initiated by Rab5 eventually triggers recruitment of Rab7 that promotes inactivation of Rab5, further acidification and formation of intraluminal vesicles and switch from PI3P to PI3,5P.

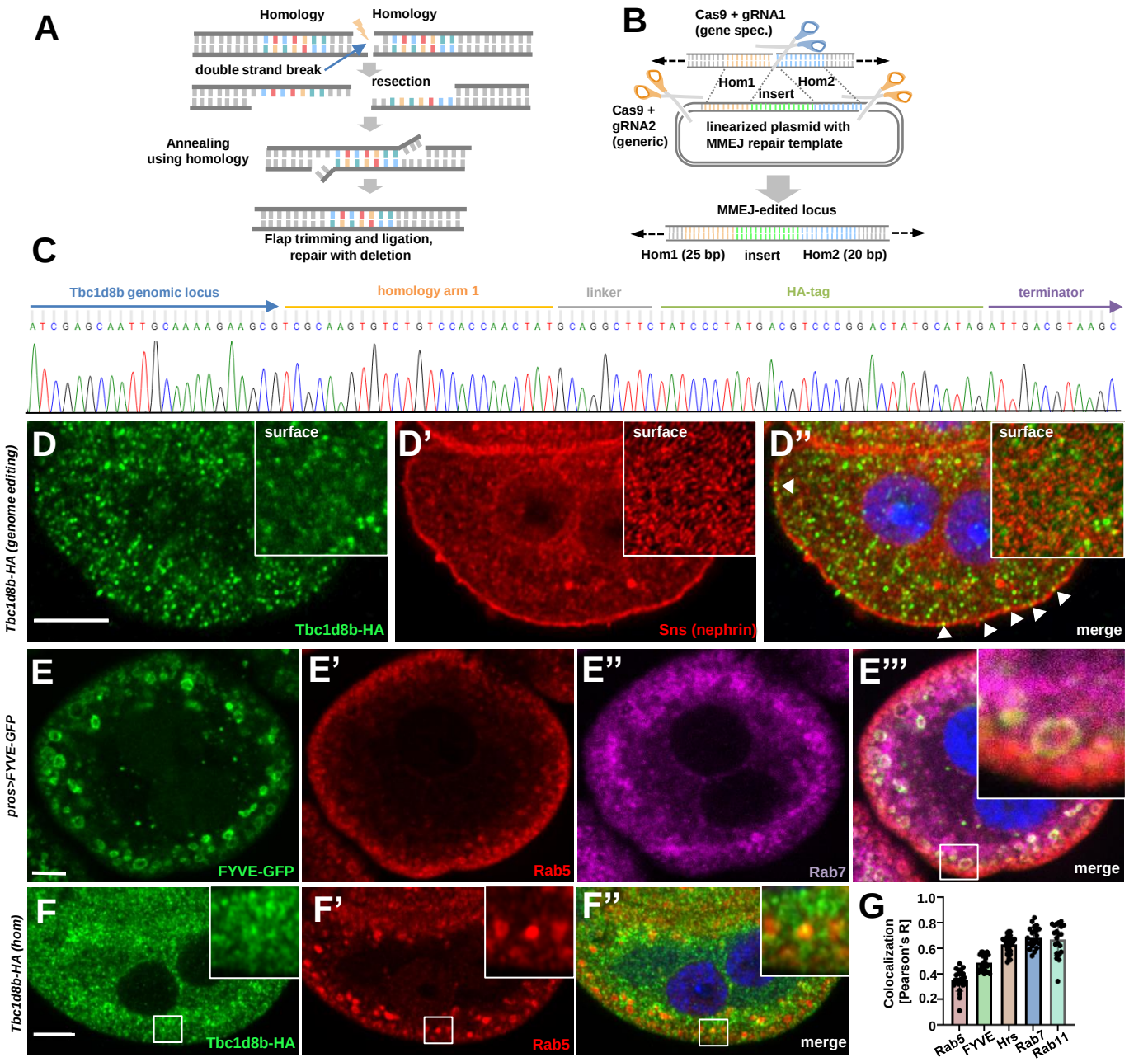

Supplemental Figure 3: Microhomology-mediated end joining and localization of Tbc1d8b.
(A) Schematic illustrates function of microhomology-mediated end joining (MMEJ). A double strand break is repaired by annealing of two homologous regions while the interjacent sequence is deleted.
(B) Schematic indicates principle of MMEJ-mediated genome editing. Two gRNAs are injected together: a generic gRNA (yellow) releases a linearized template with short homologies left and right of the double strand break caused by the gene-specific gRNA (blue). Repair results in insertion of the sequence between the homologies (green).
(C) Sanger trace confirms successful MMEJ-mediated knock-in of an HA-tag in frame into the C-terminus of the *Tbc1d8b* locus.
(D-D'') Nephrocytes from animals carrying Tbc1d8b-HA homozygously show a regular staining of slit diaphragm protein nephrin (Sns, inset shows tangential section). This suggests the tagged protein is functional. Marginal colocalization of nephrin (Sns) and Tbc1d8b-HA is observed on the surface (arrowheads).
(E-E''') A nephrocyte expressing FYVE-GFP is co-stained for early endosomal marker Rab5 and late endosomal marker Rab7. The FYVE-GFP reporters apparently localizes to an intermediate compartment with partial overlap. Nuclei are marked by Hoechst 33342 in blue here and throughout the figure.
(F-F'') Nephrocytes expressing *Tbc1d8b-HA* reveal partial colocalization of the transgene with Rab5 (magnified inset).
(G) Quantitation of colocalization in nephrocytes between Tbc1d8b-HA generated by genome editing and various endsomal compartment markers from immunofluorescence is shown (analogous to panel F and Fig. 3F-I, n = 7-10 animals per staining). Pearson's R coefficient ranges from -1 (mutual exclusion) to +1 (complete colocalization).

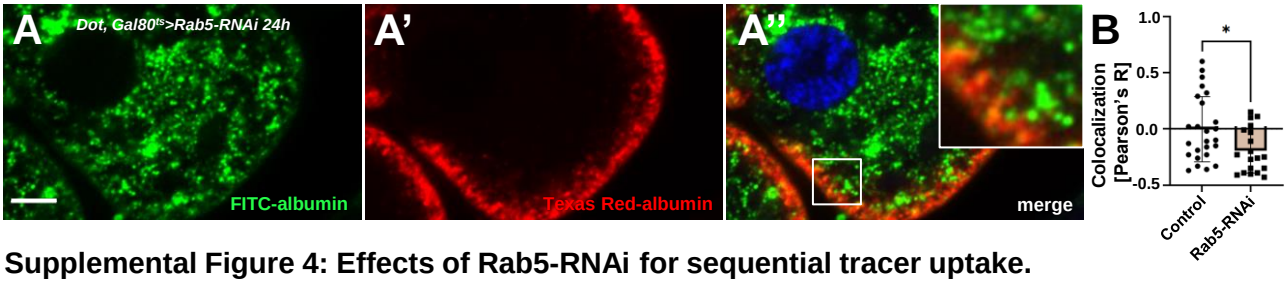

Supplemental Figure 4: Effects of Rab5-RNAi for sequential tracer uptake.
(A-A'') Sequential tracer endocytosis in nephrocytes expressing Rab5-RNAi shows diffuse localization of the first tracer and decreased colocalization.
(B) Quantitation of data expressed as Pearson's correlation coefficient (mean ± standard deviation, n=10-12 animals per genotype, $P<0.05$) supports decreased colocalization.

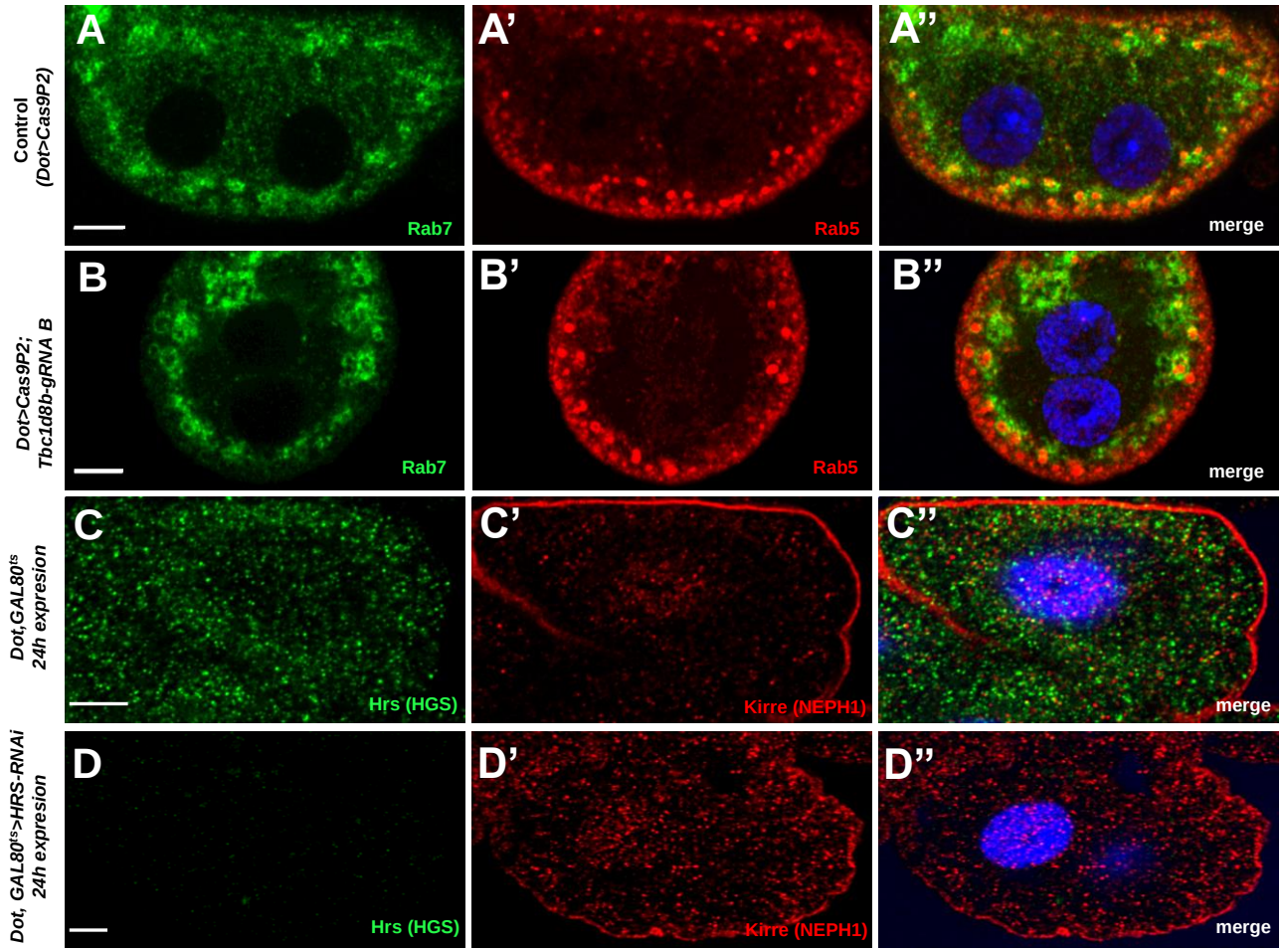

Supplemental Figure 5: Rab5- and Rab7-staining in Tbc1d8b-LOF and validation of Hrs knockdown and antibody.

(A-B'') Confocal microscopy images of nephrocytes stained for endosomal markers Rab5 and Rab7. The endosomal markers localize in concentric circular layers with Rab7 showing greater distance to the cell surface. We did not observe an overt difference of the staining pattern comparing control (A-A'') to conditional CRISPR/Cas-mediated loss-of-function of Tbc1d8b (B-B''), suggesting that overall endosomal architecture is not disrupted.

(C-C'') Signal from Hrs-staining is diffuse and fine vesicular in the cell.

(D-D'') The signal from anti-Hrs is lost in nephrocytes expressing *Hrs*-RNAi (24h on 31°C) confirming the specificity of the signal and successful knockdown of *Hrs*. Kirre shows mislocalization upon silencing.

A

```
H.sapiens       MWLKPEEVLLKNALKLWLMERSNDYFVLQRRRGYGEEGGGGLTGLLVGTLDSVLDSTAKV   60
M.musculus      MWLKPEEVLLKNALKLWLMERSNEYFVLQRRRGYGEEGGGGLTGLLVGTLDSVLDSTAKV   60
D.melanogaster  MWIQPKELLLPS--AFWIAEMHSRYFVLQKRRGHGESRG--FGSMLVGTYDSVMNT--KP   54

H.sapiens       APFRILHQTPDSQVYLSIACGANREEITKHWDWLEQNIMKTLSVFDSNEDITNFVQGKIR   120
M.musculus      APFRILHQTPDSQVYLSIACGANREEITKHWDWLEQNIMKTLSVFDSNEDITNFVQGKIR   120
D.melanogaster  APYRILHQTPSSEVSYEIAIGITQDEIVKDWEWLKANLFKVLDEMENEDEVTNFTICKIQ   114

H.sapiens       GLIAEEGKHCFAKEDDPEKFREALLKFEKCFGLPEKEKLVTYYSCSYWKGRVPCQGWLYL   180
M.musculus      GLIAEEGKQSFAKEDDPEKFREALLKFEKSFGLPEQEKLVTYYSCSYWRGRVPCQGWLYL   180
D.melanogaster  SLYTQNNQDD---TGESADFKVMKSKFRQIFKMPEEERLVISYSATYVKNKIPRQGQLYI   171

H.sapiens       STNFLSFYSFLLGSEIKLIISWDEVSKLEKTSNVILTESIHVCSQGENHYFSMFLHINQT   240
M.musculus      STNFLSFYSFLLGSEIKLIISWDAISKLEKTSTVILTESIHVCSQGENHYFSMFLHINET   240
D.melanogaster  SLNHVCFYSYMLGQEIKRIIRFAELEDISRNANTIYLKTTN----NMTYNFTMLFNASDA   227

H.sapiens       YLLMEQLANYAIRRLFDKET---FDNDPVLY-------NPLQITKRGLENRAHSEQFNAF   290
M.musculus      YLLMEQLANYAIKRLFDKET---FDNDPVLD-------DPLQITKRGLEYRAHSEQFKAF   290
D.melanogaster  HLLIEQLNKMAIQQLIHDPDSPVVDHDTSNFSRLGSKTSKKPVLLRDLTARQKSEEFRIY   287

H.sapiens       FRLPKGESLKEVHECFLWVPFSHFNTHGKMCISENYICFASQDGNQCSVIIPLREVLAID   350
M.musculus      FRLPKEETLKEVHECFLWVPFSHFSSHGKMCISENYICFASQDGNLCSVIIPLREVLAID   350
D.melanogaster  FRLPQSEIIDGKIKANIWTPYSKRFNSGFIYLSPNFFCFRSDVKDLVSVVIPMKTIKSVE   347

H.sapiens       KTNDSSKSV----IISIKGKTAFRFHEVKDFEQLVAKLRLRCGAASTQYHDISTELAISS   406
M.musculus      KTDDSNHSV----IISIKGKTAFRFSELKDFEQLVAKLRLKCRAASTQ-DDVSTEVAVSS   405
D.melanogaster  KKDDGQQHFENQIVIITSENVPFMFAHIVDRAVLISKITDLLARV---------HVPLSR   398

H.sapiens       ESTEPSDNFEVQSLTSQRECSKTVNTEALMTVFHPQNLETLNSKMLKEKMKEQSWKILFA   466
M.musculus      DSTGPSENFEEQPLTCPKECSKTVNTEALMTVFHPQNLENLDSKMLKEKMKEQSWNILFS   465
D.melanogaster  ER----AKYDIS----------WSKQTALMNTFKTQFSA---EIIQKQEEKMVRWEAHFR   441

H.sapiens       ECGRGVSMFRTKKTRDLVVRGIPETLRGELWMLFSGAVNDMATNPDYYTEVVEQSLGT-C   525
M.musculus      ECGRGVSMFRTKKTRDLVVRGIPETLRGELWMLFSGAVNDMATNPGYYAEVVEQSLGT-S   524
D.melanogaster  DFGRGIGMFRTTDVINLIVEGIPDKLRQEIWLIFSGAIHDKEMNPGLYEDLVEKAACIKN   501

H.sapiens       NLATEEIERDLRRSLPEHPAFQSDTGISALRRVLTAYAYRNPKIGYCQAMNILTSVLLLY   585
M.musculus      NLATEEIERDLRRSLPEHPAFQSDTGISALRRVLTAYAYRNPKIGYCQAMNILTSVLLLY   584
D.melanogaster  CFAHDEIDRDLPRSLPEHPAFQSTDGIGALRRVLQAYALRNPQVGYCQAMNIVSSVFLLF   561

H.sapiens       AKEEEAFWLLVAVCERMLPDYFNRRIIGALVDQAVFEELIRDHLPQLTEHMTDMTFFSSV   645
M.musculus      AKEEEAFWLLVAVCERMLPDYFNRRIIGALVDQAVFEELIRDHLPQLTDHMTDMTFFSSV   644
D.melanogaster  CDEENAFWMLASLCENLLPDYYKDKVVGAQIDQGVLNELVETHLPDLHGHLEQLGVIKMI   621

H.sapiens       SLSWFLTLFISVLPIESAVNVVDCFFYDGIKAILQLGLAILDYNLDKLLTCKDDAEAVTA   705
M.musculus      SLSWFLTLFISVLPIESAVNVVDCFFYDGIKAILQLGLAILDYNLDKLLTCKDDAEAVTA   704
D.melanogaster  SISWFLTIFMSVISYESSLHILDCFFYEGAKIIFMISLQITIENNRDKLLICQDDGEAMLV   681

H.sapiens       LNRFFDNVTNKDSPLPSNVQQGSNVSDEKTSHTRVDITDLIRESNEKYGNI-RYEDIHSM   764
M.musculus      LNRFFDNVINKDSPLPSNVQQGSNISNEKSDHTKVDITDLIKESNEKYGSI-RYEDIHSM   763
D.melanogaster  LQNYLEGVYNPEYQVPPTTDKRKMERKVQ----TQTVQTLIHEAYTKFGEDITQQRIEEL   737

H.sapiens       RCRNRLYVIQTLEETTKQNVLRVVSQDVKLSLQELDELYVIFKKELF-----LSCYWKCLG   819
M.musculus      RCRNRLYVIQTLEETTKQNVLRVVSQDVKMSLQELDELYVIFKKELF-----ISCYWYLS   818
D.melanogaster  RNKHRRLTMRQFDIDNEKTIVKAYVQNPYFNRSELHMLLTIIREEKHALKSLQQQQQKVQ   797

H.sapiens       CPVLK--------------HHDPSLPYLEQYQIDCQQFRALYHLLSPWAHSANKDSLALW   865
M.musculus      CPGLK--------------HHDPSLPYLEQYQIDCQQFRVLYHLLSPWAHSANRDSLALW   864
D.melanogaster  CPLSETPQLVPQSTSRPIQDAGASGGRYEAYSVSYEVFHTLFTELTPWRKCVSVD-IGEK   856

H.sapiens       TFRLLDENSDCLINFKEFSSAIDIMYNGSFTEKLKLLFKLHIPPAYTEVKSKDASKGDEL   925
M.musculus      TFRLLDENSDCLINFKEFSSAIDIMYNGSFTDKLKLLFKLHIPPAYTEVMSKTSSKGDEL   924
D.melanogaster  LFRLTDKKGTGVLDFGQLINALGLVCSNKNMEKLKLLYVLHLPPLLSKAEIERSRRPRPR   916

H.sapiens       SKEEL--LYFSQLHVSKPANEKEAESAKHSPEKGKGKIDIQAYLSQWQDELFKKEENIKD   983
M.musculus      STEEL--LYFSQLQVSKPADEKETESGRNSPEKGKGKIDIQAYLSQWQDELLKKEETIKD   982
D.melanogaster  TKDDAEEAFEAEDFFD----NDASESMEALPSPSDHNFDADDFA------LISATQHLHN   966

H.sapiens       LPRMNQSQFIQFSKTLYNLFHEDPEEESLYQAIAVVTSLLLRMEEVGRKLHSPTSSAKGF   1043
M.musculus      LPRMNQSQFIQFSKTLYNLFHEDPEEESLYQAIAIVTNLLLLRMEEVGRKLHSPASSAST-   1041
D.melanogaster  LAGISGNTFMDLSRTPNLSVNSN--TSSLAHRSSTFYVDLPGFQDLGAARITPPEAGVG-   1023

H.sapiens       SGTVC-GS-------------------------------------------------------   1050
M.musculus      ----A-RD-------------------------------------------------------   1044
D.melanogaster  -ADVVAGAASSAAADHMLLNVETISNFSQISDLVAATRLERVDSNATDLRSLGSLGYLLD   1082

H.sapiens       ----GGPSEE-----------------------------------------------------   1056
M.musculus      ----SGPSEG-----------------------------------------------------   1050
D.melanogaster  QPDEGASNSQHSIPHMRKENFQLLWRSIIEIMGLVQDEEMQRAYENLLELGNSNIKKEPS   1142

H.sapiens       -------------------------------------------------KTGSHLEKDPC   1067
M.musculus      -------------------------------------------------NAESSVKKDLP   1061
D.melanogaster  LESFTQLNMGGDEQPDSNGNPTTPAPEPIGTTRLFVALEEELRQASGKSRTTTTSSGDSS   1202

H.sapiens       SFREEPQWSFAFEQILASLLNEPALVRFFEKPIDVKAKLENARISQLRSRTKM-      1120
M.musculus      SPREEHQWSFAFEQILASLLNEPALVRFFERPLDLKAKLENAKSSQLRSRTKM-      1114
D.melanogaster  STNISESWHISITQFIATVLTVNSIVRGFQTPIQISEQIEQLQKKRKKCLSTNY      1256
```

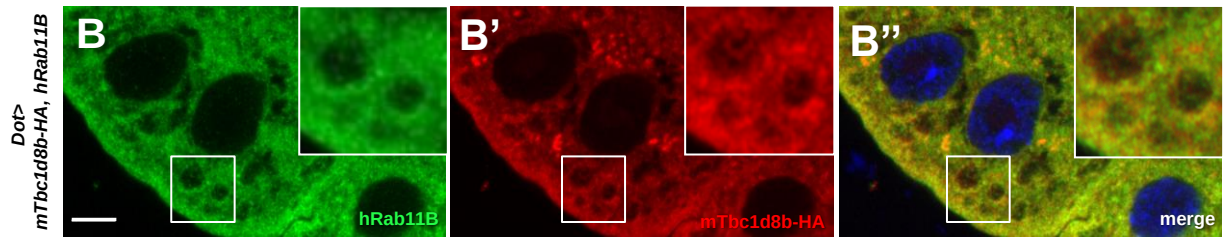

Supplemental Figure 6: Alignment of human, murine and *Drosophila Tbc1d8b* and coexpression with human *Rab11B*.

(A) Protein sequences are aligned using Clustal Omega (https://www.ebi.ac.uk/Tools/msa/clustalo/).

(B) Co-expression of human *Rab11B* and murine *Tbc1d8b-HA* in *Drosophila* in nephrocytes results in partial colocalization of both expressed transgenes.

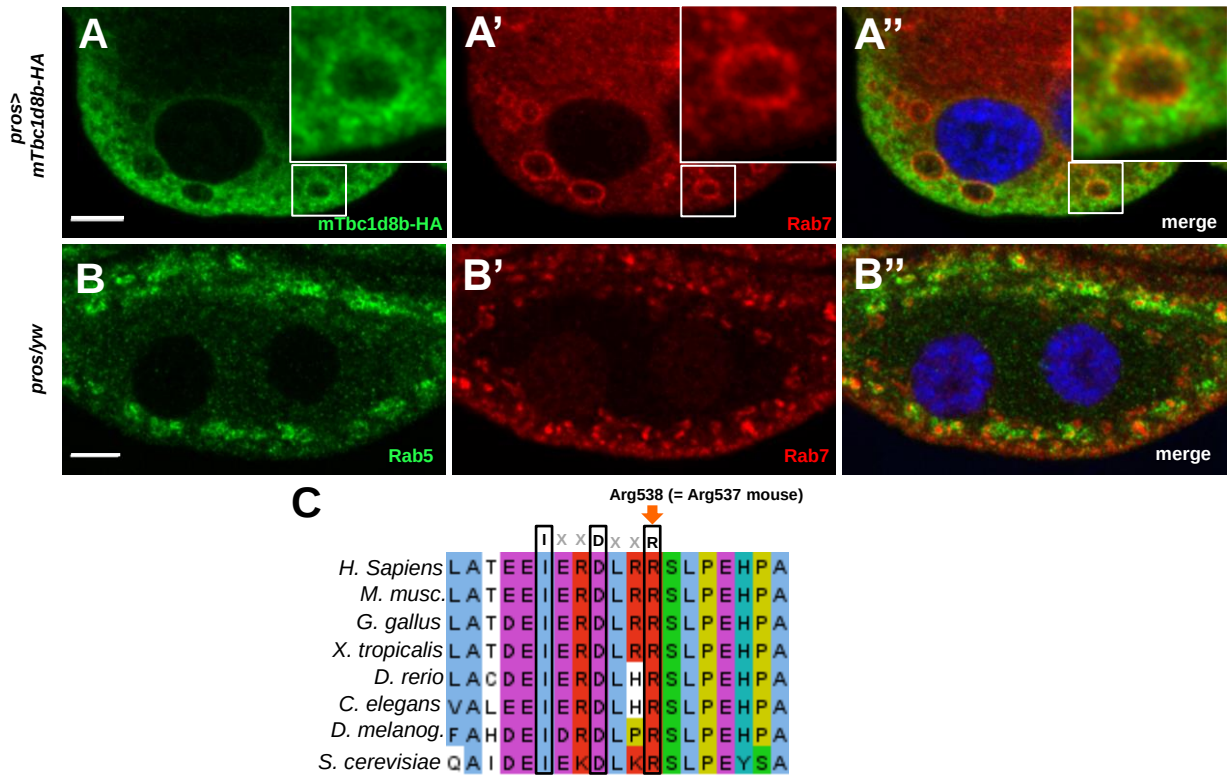

Supplemental Figure 7: Overexpression studies of murine Tbc1d8b.
(A-A'') Staining of nephrocytes overexpressing murine *Tbc1d8b*-HA reveals localization of the mammalian protein includes the outer membrane of enlarged endosomes.
(B-B'') Control nephrocytes occasionally show Rab5 within the larger Rab7 positive vesicles but no extensive colocalization on the outer membrane of late endosomes.
(C) Alignment of TBC1D8B amino acid sequences around residue Arg538 is shown. The sequence reveals a conserved IXXDXXR motif. This suggests this residue is the catalytically essential arginine finger.

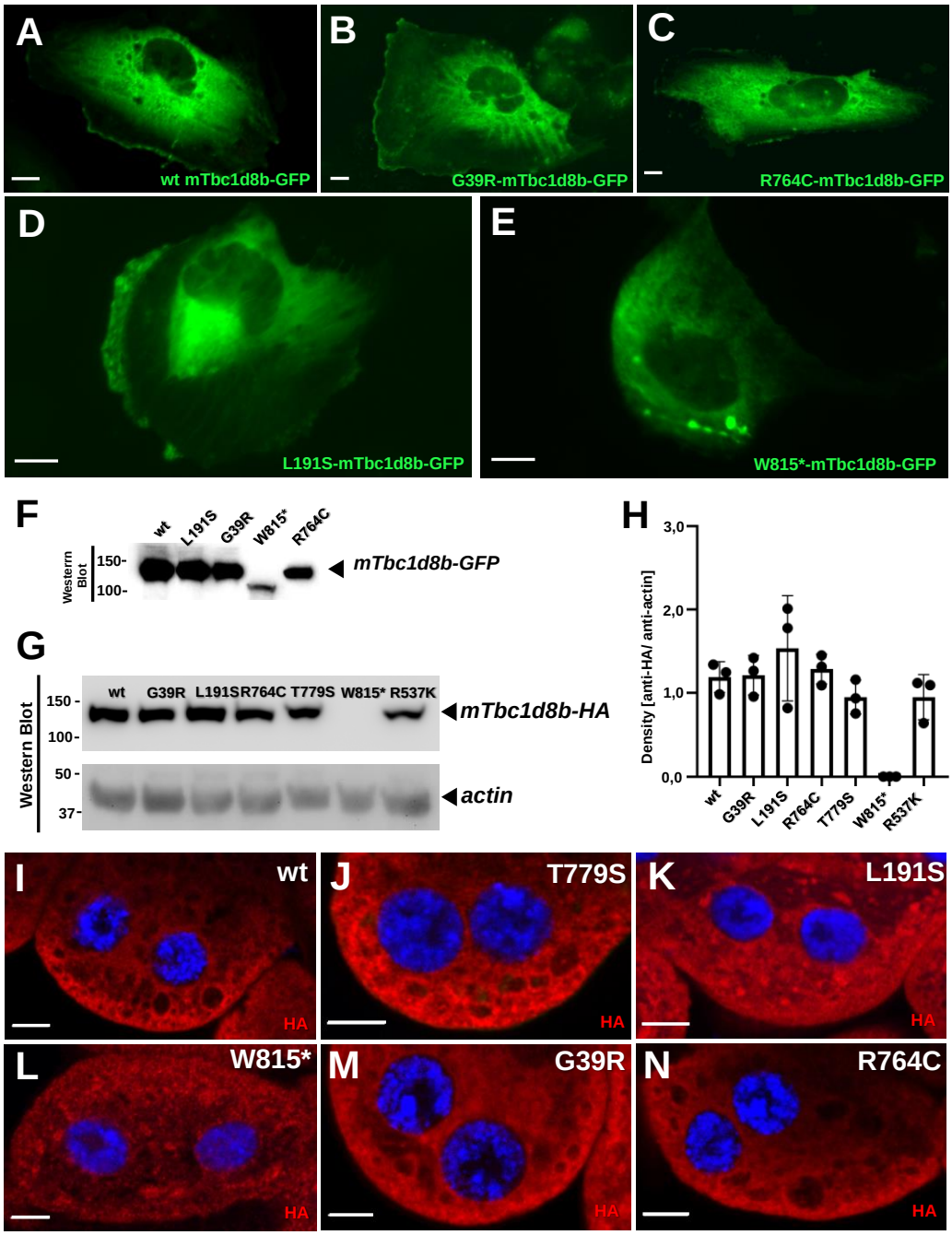

Supplemental Figure 8: Patient-derived mutations in *TBC1D8B*.

(A-E) Cultured podocytes were transiently transfected with GFP-tagged variants of m*Tbc1d8b-HA* and reporter fluorescence revealed a cytosolic localization (A-D) with the exception of the truncating mutant W815* (E). Scale bars represent 10 µm. Brightness was adjusted for each image to ensure proper image quality.

(F) Cultured HEK293T-cells were transiently transfected with GFP-tagged variants of m*Tbc1d8b*. Immunoblotting confirms decreased expression of the truncating variant in a mammalian cell system.

(G) Immunoblotting from third instar larve expressing the indicated variants of mTbc1d8b-HA under control of *prospero* GAL4 (31°C) indicates equal expression except for the truncating mutant W815*.

(H) Quantitation of the density of (G) expressed as ratio (anti-HA/anti-actin) reveals no statistical significant difference except for W815*.

(I-N) Staining the corresponding genotypes from for HA-tag in nephrocytes reveals the subcellular localization of the respective transgenes. Wild type mTbc1d8b localizes partially in the cytosol but also in vesicles at the cell periphery (I). Mutant transgenes locate in smaller vesicles across the cell in a mildly divergent pattern for L191S (K) and W815* (L). T779S (J), G39R (M) and R764C (N) did not show a significantly different staining pattern. Laser power was elevated for W815* due to protein lower abundance.

Construct	Direction	Primer sequence
G39R-mTbc1d8b (no tag)	Forward	TACGGGGAAGAAGGAAGAGGGGACTTACAG
G39R-mTbc1d8b (no tag)	Reverse	CTGTAAGTCCCCCTCTTCCTTCTTCCCCGTA
L191S-mTbc1d8b (no tag)	Forward	CAACTTTCTGAGCTTCTATTCCTTCTCGCTAGGATCAGAAATTA
L191S-mTbc1d8b (no tag)	Reverse	TAATTTCTGATCCTAGCGAGAAGGAATAGAAGCTCAGAAAGTTG
R764C-mTbc1d8b (no tag)	Forward	CTATGAAGATATACATAGCATGTGCTGTCGAAATAGGTTGTATGT
R764C-mTbc1d8b (no tag)	Reverse	ACATACAACCTATTTCGACAGCACATGCTATGTATATCTTCATAG
W815*-mTbc1d8b (no tag)	Forward	GAGCTGTTTATATCTTGTTATTGATATTTGAGTTGTCCAGGATTGAA
W815*-mTbc1d8b (no tag)	Reverse	TTCAATCCTGGACAACTCAAATATCAATAACAAGATATAAACAGCTC
mTbc1d8b-variants in HA-backbone (except for W815*)	Reverse	GACGTCATAGGGATAGAAGCCTGCCATCTTGGTTCTAGACCTTAGC
W815*-mTbc1d8b-HA (no tag W815* into HA-backbone)	Reverse	GACGTCATAGGGATAGAAGCCTGCATAACAAGATATAAACAGCTCTTTCTTAAAAATG
R537K-mTbc1d8b-HA	Reverse	CGGGCAGAGATTTACGCAAATCACGCTCAATTTCTTC
R537K-mTbc1d8b-HA	Forward	TTTGCGTAAATCTCTGCCCGAACATCCAGCA
generic primer for mTbc1d8b variants	Forward	GTACAAAAAAGCAGGCTTCACCATGTGGCTGAAGCCCGAGGA
generic primer for mTbc1d8b variants	Reverse	CTTTGTACAAGAAAGCTGGGTCCTATCACATCTTGGTTCTAGACCTTAG
human Rab11B	Forward	GTACAAAAAAGCAGGCTTCACCATGGGGACCCGGGACGAC
human Rab11B	Reverse	CTTTGTACAAGAAAGCTGGGTCCTATCACAGGTTCTGGCAGCAC
Tbc1d8b gRNA B pCFD5_w	Forward	GCGGCCCGGGTTCGATTCCCGGCCGATGCAGTGGGCGCCCAAATCGATCAGTTTTAGAGCTAGAAATAGCAAG
Tbc1d8b gRNA B pCFD5_w	Reverse	ATTTTAACTTGCTATTTCTAGCTCTAAAACCGTCTCTTCTGCAGGACAAATGCACCAGCCGGGAATCGAACCC
Tbc1d8b-HA MMEJ repair template backbone	Forward	AGGACCCAGCTTTCTTGTACAAAG
Tbc1d8b-HA MMEJ repair template backbone	Reverse	CCTGTACTGATCTTGCGTTAATGCATGGTGAAGCCTGCTTTTTTGTAC
Tbc1d8b-HA MMEJ repair template insert PCR 1	Forward	CATTAACGCAAGATCAGTACAGGTCGCAAGTGTCTGTCCACCAACTATGCAGGCTTCTATCCCTATGACGTCCCGGACTATGCATAGATTGACGTAAGCTAGTCTAGACG
Tbc1d8b-HA MMEJ repair template insert PCR 1	Reverse	AGATCGTCGGCAAGAGACATCCACTT
Tbc1d8b-HA MMEJ repair template insert PCR 2	Forward	AAGTGGATGTCTCTTGCCGACGATCTTTACTAGTGCTCTTCTATAACT
Tbc1d8b-HA MMEJ repair template insert PCR 2	Reverse	CTTTGTACAAGAAAGCTGGGTCCTCATTAACGCAAGATCAGTACAGGGACTATGATTATTCAGTAATCCATGACGTTGCGTAATCACGA
Tbc1d8b-HA MMEJ pCFD4 for guide RNAs	Forward	TATATAGGAAAGATATCCGGGTGAACTTCGTATGATTATTCAGTAATTGGGTTTTAGAGCTAGAAATAGCAAG
Tbc1d8b-HA MMEJ pCFD4 for guide RNAs	Reverse	ATTTTAACTTGCTATTTCTAGCTCTAAAACGTACTGATCTTGCGTTAATGCGACGTTAAATTGAAAATAGGTC
Tbc1d8b-HA MMEJ sequencing primer	Forward	AGAGGAGCTTCGTCAGGCGA
Tbc1d8b-HA MMEJ sequencing primer	Reverse	TTACTAGAGGATCGTACGGATCTG
Tbc1d8b (D.m.) null allele sequencing primer	Forward	ATAAGCCGACTCTAAAGGTGAAC
Tbc1d8b (D.m.) null allele sequencing primer	Reverse	CTCCAGATGGCCGTGCAAATC
Tbc1d8b gRNA A on X pCFD5_w	Forward	GCGGCCCGGGTTCGATTCCCGGCCGATGCACTACTACAAGGATAAAGTGGGTTTTAGAGCTAGAAATAGCAAG
Tbc1d8b gRNA A on X pCFD5_w	Reverse	ATTTTAACTTGCTATTTCTAGCTCTAAAACCGTGATTCCCCATGGCCACGTGCACCAGCCGGGAATCGAACCC

Supplemental Table 1: Primer sequences